Reductive amination cascades in cell-free and resting whole cell formats for valorization of lignin deconstruction products

Authors: Priyanka Nain, Roman M. Dickey, Vishal Somasundaram, Morgan Sulzbach, and Aditya M. Kunjapur*

Affiliations:

Department of Chemical & Biomolecular Engineering, University of Delaware, Newark, DE 19716

*Correspondence: Correspondence to A.M.K. at kunjapur@udel.edu

Abstract

The selective introduction of amine groups within deconstruction products of lignin could provide an avenue for valorizing waste biomass while achieving a green synthesis of industrially relevant building blocks from sustainable sources. Here, we built and characterized enzyme cascades that create aldehydes and subsequently primary amines from diverse lignin-derived carboxylic acids using a carboxylic acid reductase (CAR) and an ω-transaminase (TA). We report a detailed characterization of two reaction formats - cell-free biocatalysis and resting whole-cell biocatalysis - using the conversion of vanillate to vanillyl amine as model chemistry. We showed that resting whole-cell reactions could be competitive with cell-free reactions (97% and 70% yields, respectively) while avoiding steps of cell lysis, purification, and cofactor supplementation. We also demonstrated the recyclability of resting whole cells for multiple batches of catalysis without significant loss in productivity. Finally, we used the knowledge gained from this study to produce several amines from carboxylic acid precursors using one-pot biocatalytic reactions. These results expand our knowledge of these industrially relevant enzyme families to new substrates and contexts for environmentally friendly and potentially low-cost synthesis of diverse aryl aldehydes and amines.

Keywords: lignin, valorization, cell-free, whole-cell biocatalysis, amines, carboxylic acid reductase, transaminase

Introduction

Lignin is the largest natural source of aromatic compounds and possesses significant potential as an alternative to petroleum-based feedstocks for materials production. However, a staggering 98% of lignin is burned as waste each year (Fache et al., 2014; Su et al., 2022; Sun et al., 2018; Upton and Kasko, 2016). Although a barrier to the utilization of lignin is its complexity, technical advances made over the last few decades have led to the design of chemical and biological deconstruction processes that funnel lignin toward a limited range of building blocks (José Borges Gomes et al., 2020; O'Dea et al., 2022; Schutyser et al., 2018; Wang et al., 2019a). Some of these building blocks have features that are attractive for industrial or pharmaceutical applications but importantly lack an amine group (Holmberg et al., 2016b; Holmberg et al., 2016a; Wang et al., 2018b). Aryl amines are desirable for a range of applications spanning carbon capture (Hallenbeck and Kitchin, 2013), biobased polyamine vitrimers (Dhers et al., 2019), thermosets (Lee et al., 2016), and the pharmaceutical industry (Yuan et al., 2023). Such chemicals are especially desirable when derived from bio-renewable sources to minimize the environmental impact of the manufacturing process (Fache et al., 2016; Guggari et al., 2023; Hakkarainen et al., 2020). However, new methods are needed to introduce amine groups within lignin deconstruction products as amine formation can be synthetically intensive. For example, the transformation of aldehydes to primary amines (*e.g.*, the conversion of vanillin to vanillyl amine) by a synthetic reductive amination pathway relies on multi-step reactions, low atom economies, and potentially hazardous chemicals (Abdel-Magid et al., 1996; Podyacheva et al., 2019).

We hypothesized that we could convert some of the products of the biological degradation (Molinari et al., 2023), or oxidative deconstruction (Cui et al., 2021; Rahimi et al., 2014) of lignin, which can be aryl carboxylic acids or aldehydes, to their corresponding amines by constructing a

one-pot biocatalytic cascade (**Figure 1a**). This one-pot biocatalytic cascade would feature carboxylic acid reductases (CARs, E.C. 1.2.1.30) and ω-transaminases (TAs, E.C.2.6.1.x). CAR enzymes catalyze the two-electron reduction of a broad range of carboxylic acids to their corresponding aldehydes at the cost of ATP and NADPH (Butler and Kunjapur, 2020). These multidomain enzymes first catalyze the adenylation of carboxylic acids using ATP in the N-terminal adenylation domain, next form a thioester on a phosphopantheinyl swinging arm in the thiolation domain, and finally catalyze the formation of an aldehyde at the expense of NADPH in the C-terminal reduction domain. TAs are pyridoxal 5'-phosphate (PLP)-dependent enzymes that have previously been applied to reversibly catalyze amination by transferring an amine group from an amine donor to the substrate aldehyde or ketone through a pyridoxamine 5'-phosphate (PMP) intermediate (Höhne and Bornscheuer, 2009; Ngo et al., 2022; Rocha et al., 2019). Recently, we reported bioprospecting of diverse CAR enzymes and their coupling to the well-known ω-TA from *Chromobacter violaceum* (cvTA) to build a one-pot cascade for highly selective and efficient conversion of deconstruction product from polyethylene terephthalate (PET) to mono-and diamines (Gopal et al., 2023). In this paper, we sought to investigate whether we could extend this concept to a different set of chemistries derived from lignin, and we also wondered whether we could employ resting whole cell biocatalysts that express the cascade and compare them to cell-free biocatalysis. To our knowledge, these enzymes have not been comprehensively analyzed for their substrate specificity towards distinct variations of syringol and guaiacol units.

Here, we report the design of enzyme cascades that couple CAR and amine-transferring enzymes for the synthesis of vanillyl amine (1c), syringylamine (2c), cinnamylamine (3c), 4-hydroxy-3-methoxy cinnamylamine (4c), and 3-(4-hydroxy-3-methoxyphenyl) propylamine (5c). Our whole cell biocatalysis work utilizes a unique strain of *Escherichia coli* that exhibits reduced

oxidation and reduction of aryl aldehydes (ROAR) (Butler et al., 2023), which recently built upon our prior work that focused solely on mitigating aldehyde reduction in *E. coli* (Kunjapur et al., 2014). Overall, our work fills a void in the existing arsenal of biomass upcycling approaches, thereby enhancing the prospects for efficient valorization of lignin deconstruction streams.

Material and Methods

Reagents

The following compounds were purchased from Millipore Sigma: kanamycin sulfate, dimethyl sulfoxide (DMSO), potassium phosphate dibasic, potassium phosphate monobasic, magnesium sulfate, calcium chloride dihydrate, glycerol, tris base, glycine, 4-(2-hydroxyethyl)-1-piperazineethanesulfonic acid (HEPES), Adenosine triphosphate (ATP), vanillate, trans-cinnamic acid, ferulic acid, and trans cinnamaldehyde, syringaldehyde, vanillin, benzaldehyde, 4-hydroxy-3-methoxy cinnamaldehyde, vanillyl amine and KOD XTREME Hot Start and KOD Hot Start polymerases. Syringate was purchased from Merck Millipore. 3-(4-hydroxy-3-methoxyphenyl) propanal was procured from AA Blocks. 3-(4-Hydroxy-3-methoxyphenyl) propionic acid was purchased from Chemspace. D-glucose was purchased from TCI America. Agarose and ethanol were purchased from Alfa Aesar. Acetonitrile, sodium chloride, LB Broth powder (Lennox), and LB Agar powder (Lennox), were purchased from Fisher Chemical. Taq DNA ligase was purchased from GoldBio. Phusion DNA polymerase and T5 exonuclease were purchased from New England BioLabs (NEB). Sybr Safe DNA gel stain was purchased from Invitrogen. NADPH (tetrasodium salt) was purchased from Santa Cruz Biotechnology. Anhydrotetracycline was purchased from Cayman Chemical. IPTG was purchased from Thermo Scientific (USA). Triethylamine, sodium bicarbonate, hydrochloric acid, magnesium sulfate, and sodium hydroxide were purchased from Fisher Scientific.

Cloning and Purification

Cloning, expression, and purification of carboxylic acid reductases

Molecular cloning and vector propagation were performed in *E. coli* DH5α (NEB). *Escherichia coli* strains and plasmids used are listed in **Table S1**. Various pZE plasmid constructs (accession OP031608, OP031609, OP031610, OP031611, OP031612, and OP031615) containing CARs (CAR genes from *Mycobacterium avium, Segniliparus rotundus, Mycobacterium marinum, Neurospora crassa, Trichoderma reesei,* and *Aspergillus fumigatus*) and Sfp from *Bacillus Subtilis* were transformed in *E. coli* ROAR cells. Sfp is essential for the post-translational activation of CAR apoenzyme to the holoenzyme. Nevertheless, srCAR and bsSfp were also cloned in pDuet vector under separate T7 promoters as well. All plasmids were verified by Sanger sequencing.

For expression, all CAR plasmids were transformed into *E. coli* ROAR (Butler et al., 2023) for whole cell biocatalysis purposes and BL21 (DE3) for purification. 250 mL of LB-Lennox medium (LBL: 10 g/L bacto tryptone, 5 g/L sodium chloride, 5 g/L yeast extract), in 1 L baffled flasks were supplemented with 5 mM glucose, 2.5 mM $MgSO_4$, and 30 µg/mL kanamycin (Fisher Scientific) was inoculated with 1% of saturated overnight culture and induced at mid-exponential phase (OD600 0.5-0.8) with 0.1 µg/mL anhydrotetracycline (ATC, Cayman Chemical). The cultures were grown at 37 °C until the induction followed by a 5 h growth at 30 °C and left at 18 °C overnight. The recombinant protein expressing cells were harvested by centrifugation at 4°C for 10 min at 7176 × *g*. The cell pellet was washed twice with 0.1 M HEPES (pH 7.5) and immediately utilized/stored at -80 °C for future uses.

For purification, the freshly harvested cells were resuspended in Nickel-binding buffer (100 mM HEPES pH 7.5, 250 mM NaCl, 10 mM imidazole, 10% glycerol, 10 mM magnesium

chloride). After being sonicated, the cells were centrifuged at 17,100 × *g* for 1 h, and cleared supernatant was further sterile filtered through a 0.22 µm syringe filter (Merck Millipore). An AKTA Pure fast protein liquid chromatography (FPLC) system (GE Healthcare) containing a Ni-Sepharose affinity chromatography (HisTrap HP, 5 mL) column with isocratic binding, wash, and elution steps was used for purification. The pumps and data acquisition were controlled using Unicorn™ 7.3 software (GE Healthcare). Final elution was carried out at 250 mM imidazole. Purified fractions were pooled, concentrated, and dialyzed against Dialysis Buffer (100 mM HEPES pH 7.5, 300 mM sodium chloride, 10% glycerol, and 10 mM magnesium chloride hexahydrate) with 30 kDa molecular weight cutoff centrifugal filter (Amicon Ultra, Millipore). Purified protein fraction was stored in Eppendorf tubes which were flash-frozen in ultracold ethanol and stored at -80 ºC.

Cloning, expression, and purification of ω-transaminase, L-alanine Dehydrogenase, and inorganic pyrophosphatase

The ω-transaminase (TA) from *Chromobacterium violaceum* (cvTA), *Vibrio fluvialis* (vfTA), and L-alanine dehydrogenase (AlaDH) from *Bacillus subtilis* were purchased as gene fragments from IDT and were codon optimized for expression in engineered *E. coli K-12 MG1655*. These gene fragments were cloned using Gibson Assembly into a pACYC vector containing an N-terminal His_6-tag and chloramphenicol resistance marker. The putative adenosylmethionine-8-amino-7-oxononanoate transaminase from *Xanthomonas translucens* (xtTA) was cloned using Golden Gate Assembly with the aid of the JGI. In our previous work, the inorganic pyrophosphatase gene (ecPPase) was amplified by PCR from the *E. coli* MG1655 genome and was cloned into the pACYC vector containing an N-terminal His-tag by Gibson Assembly (Gopal et al., 2023). All plasmids were transformed into *E. coli* ROAR for whole cell biocatalysis and

BL21(DE3) for purification. For high cell density expression, 250 mL of LB-Lennox medium (LB: 10 g/L bacto tryptone, 5 g/L sodium chloride, 5 g/L yeast extract) in a 1 L baffled flask was supplemented with 5 mM glucose, 2.5 mM $MgSO_4$, and an appropriate antibiotic. The high cell density flask was inoculated using 1% volume from a saturated overnight culture and induced at mid-exponential phase (OD 0.5-0.8) with 1 mM Isopropyl ß-D-1-thiogalactopyranoside (IPTG, Fisher Scientific). The cultures were grown at 37 °C until induction followed by a 5 h growth at 30 °C and left at 18 °C overnight (P1 expression). An alternative approach was also taken where the cultures were grown at 37 °C until induction followed by a 5 h growth at 30 °C (P2 expression). The recombinant protein expressing cells were harvested by centrifugation at 4 °C for 10 min at 7176 × *g*. The cell pellet was washed twice with 0.1 M HEPES (pH 7.5) and utilized immediately/stored at -80 °C for future uses.

For purification, the freshly harvested cells containing recombinant TAs were resuspended in Ni-binding buffer enriched with 400 µM PLP (TCI America). Cells were ruptured by sonication and the suspension was centrifuged at 17,100 × *g* for 1 h in an Eppendorf 5430R centrifuge and the cleared supernatant was further filtered using a 0.22 µm syringe filter (Merck Millipore). Using an imidazole gradient for protein elution, recombinant proteins were purified using Ni-Sepharose affinity chromatography (GE Healthcare). Final elution was carried out at 250 mM imidazole. Purified fractions were concentrated and dialyzed with a 10 kDa molecular weight cutoff centrifugal filter (Amicon Ultra, Millipore). Purified protein fraction was stored in Eppendorf tubes which were flash-frozen in ultracold ethanol and stored at -80 ºC.

SDS-page and western blot analysis of recombinant protein expression

Protein expression was confirmed using 10% SDS-PAGE (sodium dodecyl sulfate-polyacrylamide gel electrophoresis) in a Mini-PROTEAN gel apparatus (Bio-Rad, USA). The

media type and conditions after induction are listed in **Table S2**. About 2 mL of high cell density culture was centrifuged at 7,176 × *g*, and the pellet was lysed using silica beads in lysis buffer. After clearing cell debris by centrifugation, lysate total protein concentration was measured by a Bradford Assay, with bovine serum albumin (BSA) as a standard. Total protein from each lysate was denatured in SDS and β-mercaptoethanol prior to loading 5 μg total protein onto a 10% SDS-PAGE gel and run at 150 V for 75 min. For western blotting, proteins from SDS-PAGE were transferred to an Immobilon-E polyvinylidene difluoride membrane (EMD Millipore). The membrane after the transfer was incubated for 1 h with 5% fat-free milk in a Tris-buffered saline solution for blocking followed by 0.1 μg/mL anti-his antibodies (Proteintech) in 5% fat free milk in a Tris-buffered saline solution. After 3 washes with TBST buffer, the membrane was stained with chemiluminescent reagents (Amersham ECL Prime) to visualize the transferred protein.

Enzymatic Assays

***In vitro* assay for evaluating substrate specificity of CARs on carboxylic acids derived from lignin**

We performed *in vitro* activity assays to test the substrate scope of various CARs on lignin-derivable aromatic carboxylic acids that contain varying aryl substitution patterns. *In vitro* CAR assays were performed using 0.2 mg/mL purified CAR, a buffer containing 100 mM HEPES pH 7.5 at 30 °C, equimolar concentration of NADPH, and 1.25x ATP relative to the substrate, 10 mM $MgCl_2$, 5 mM substrate, and 5-10% v/v DMSO in 100 μL of the reaction mix. We also added 0.1 mg/mL purified inorganic pyrophosphatase from *E. coli* (ecPPase) to consume the inorganic pyrophosphate (PPi), which can lead to CAR inhibition (Kunjapur et al., 2016). Each reaction was run at a 100 μL scale in triplicate in a 96-well plate and incubated. The reactions were allowed to proceed for 24 h at 30 ºC with shaking at 1000 rpm on a plate shaker prior to quenching with

trichloroacetic acid (TCA). The reaction progress was monitored using RP-HPLC at our chosen endpoint of 24 h (see HPLC Methods). The reaction was quenched with equimolar methanol and centrifuged twice to remove any insoluble protein precipitate. The supernatant was subjected to the RP-HPLC analysis to test the CAR activity on these compounds. All the experiments were done in triplicate and the standard deviation was calculated.

***In vitro* bioconversion of lignin derivable aldehyde to amines by various TAs**

To utilize CAR-generated aldehydes as intermediates, *in vitro* assays were conducted to access the substrate range of various TAs on lignin derivable aromatic aldehyde with varying aryl substitution. *In vitro* assays were performed using 0.5 mg/mL cvTA, 100 mM HEPES pH 7.5, 5% DMSO, 5 mM substrate, 2 mM PLP (TCI Chemicals), and 20 mM isopropyl amine (*i*Pr-NH_2). Various amine donors at different molar ratios were tested in search of the best one for our substrate chemistries (e.g., *o*-xylylenediamine, *i*Pr-NH_2, alanine, and methyl benzylamine). Each reaction was run at a 100 μL scale in triplicate. The reactions were allowed to proceed for 24 h at 30 ºC with shaking at 1000 rpm on a plate shaker prior to quenching with TCA. Samples were monitored for substrate depletion using HPLC-UV after centrifugation to clear insoluble protein precipitate (see **HPLC Methods**).

***In vitro* bioconversion of model chemistry vanillate to vanillyl amine in one pot**

Bioconversion of vanillate (1a) to vanillyl amine (1c) was tested in one pot using the insights from CAR and TA bioprospecting experiments. The assay was performed in one pot using 0.1 mM HEPES pH 7.5, equimolar NADPH, and 1.25x ATP to the substrate, 10 mM $MgCl_2$, 5-10% v/v DMSO, 5 mM substrate, 4x (if otherwise mentioned) molar excess of *i*Pr-NH_2 (relative to substrate), 0.2 mg/mL srCAR, 0.1 mg/mL ecPPase, and 0.5 mg/mL cvTA. Reactions were performed in triplicate in 100 μL and incubated at 30 ºC with shaking at 1000 rpm for shaking at

plate shaker. The reactions were allowed to proceed for 24 h at 30 ºC with shaking at 1000 rpm on a plate shaker prior to quenching TCA. Samples were analyzed over HPLC-UV after centrifugation to clear insoluble protein precipitate (see **HPLC Methods**).

Preparation of whole-cell biocatalysts for vanillin synthesis

Using the insights obtained from the *in vitro* experiment, the best-acting CAR and TA were employed to produce 1c from 1a. ROAR cells were transformed with a pZE plasmid harboring srCAR and BsSfp gene to create WC1 cells (Table **S1**). The recombinant protein expressing cells were grown as mentioned in Table S1 and harvested by centrifugation at 4 °C for 10 min at 7176 × *g*. The cell pellet was washed twice with 0.1M HEPES (pH 7.5) before doing the resting and fermentative cell assays.

To assay srCAR in WC1 whole cells, we mixed resting cells concentrated to 100 mg/mL in buffer with 0.1M HEPES, pH 7.5, 100 mM glucose (for regeneration of ATP and NADPH), 10 mM magnesium chloride, 10% DMSO and 5 mM vanillate in 1 mL volume and loaded 250 µL of reaction mix in 96-deep well plates. All the 96 deep well biotransformation reactions were carried out at 1000 rpm and 30 °C on a plate shaker. Each reaction was run at a 250 µL scale in triplicate. All the biotransformation reactions were carried out at 1000 rpm and 30 °C on a plate shaker. The samples were periodically taken and used for HPLC analysis of product levels.

Preparation of whole cell biocatalysis for vanillyl amine synthesis from vanillin

ROAR cells were transformed with a pACYC plasmid harboring cvTA gene to create WC2 cells (Table **S1**). The recombinant protein expressing cells were grown as mentioned in **Table S1** and harvested by centrifugation at 4 °C for 10 min at 7176 × *g* The cell pellet was washed twice with 0.1M HEPES (pH 7.5) before doing the resting cell assays.

To assay cvTA activity in WC2 whole cells, we mixed resting cells concentrated to 100 mg/mL in buffer with 0.1 M HEPES, pH 7.5, 4x *i*Pr-NH_2, 10% DMSO and 5 mM vanillin in 250 µL reaction volumes prepared in triplicate in 96-deep well plates. All the 96 deep well biotransformation reactions were carried out at 1000 rpm and 30 °C on a plate shaker. The samples were periodically taken and used for HPLC analysis of product levels.

Whole-cell one-pot selective valorization of vanillate to vanillyl amine

Initially, WC1 (100 mg/mL) and WC2 (50 mg/mL) were incubated in a reaction mixture containing 10-100 mM glucose (for cofactor regeneration), 10 mM magnesium chloride, 10% DMSO, 4x *i*Pr-NH_2, and 5 mM vanillate. WC5 cells (ROAR cell harboring pDuet-srCAR-sfp and pAcyc-cvTA-AlaDH) were concentrated to 100 mg/mL in the assay buffer mentioned above. Each reaction was run at a 250 µL scale in triplicate. All the biotransformation reactions were carried out at 1000 rpm and 30 °C on a plate shaker or in 1.5 mL Eppendorf tubes at 250 rpm in the incubator (Infors HT Multitron Triple Incubator Shaker Unit6 - AV). The samples were periodically taken and used for HPLC analysis to evaluate vanillyl amine formation.

Whole-cell reusability

To examine the whole-cell reusability, whole cells harboring plasmid with appropriate enzyme cascade (WC1, WC2, and WC5) were harvested subsequent to high cell density expression. The resulting whole cells were mixed in assay buffer to obtain a wet biomass of 100 mg/mL, after which the reaction was performed at 30 °C with shaking at 250 rpm. Following completion of the reaction, the cells were separated from the reaction mix by centrifugation at 7176 × *g* for 10 min at 4 °C and washed twice with 1 mL of 0.1 M HEPES (pH 7.5). The recovered whole cells were then utilized in subsequent reactions, and this process was repeated up to 8 h for

WC1 (at an interval of 2 h so 4 rounds) and WC2 (at an interval of 4 h so 2 rounds), and up to 24 h for WC5 at an interval of 6 h.

Chemical Detection and Analytical Methods

HPLC Method 1: Detection of vanillate (1a), Syringate (1b), their aldehyde and amine forms

Compounds of interest were quantified using reverse-phase high-performance liquid chromatography (RP-HPLC) with an Agilent 1260 Infinity with a Zorbax Eclipse Plus-C18 column (part number: 959701-902, 5 µm, 95Å, 2.1 x 150 mm). The column temperature was maintained at 30 °C. To achieve separation, the mobile phases used consisted of solvent A/B (solvent A: water with 0.1% trifluoroacetic acid, solvent B: acetonitrile with 0.1% trifluoroacetic acid). A gradient elution was performed (A/B) with a shallow gradient from 100/0 to 80/20 for 0-10 min, subsequently a gradient from 80/20 to 70/30 for 10-12 min, followed by a gradient from 70/30 to 50/50 for 12-15 min, maintenance at 50/50 for 15-16 min, a gradient from 50/50 to 100/0 for 16 to 16.5 min, and equilibration at 100/0 for 16.5-18 min. A flow rate of 0.8 mL min^{-1} was maintained, and absorption was monitored at 265, and 280 nm.

HPLC Method 2: Detection of 4 hydroxy-3-methoxycinnamic acid (4a), its aldehyde and amine forms

RP-HPLC system and the column employed were identical to the previously described with a slight variation in the HPLC method. For these chemistries, gradient elution was performed (A/B) with a gradient transitioning from 100/0 to 70/30 for 0-10 min. Subsequently, from 10 -12 min the gradient was slightly increased from 70/30 to 60/40, followed by a very shallow gradient

from 60/40 to 50/50 for 12-22 min with a rise in B every second minute, maintenance at 50/50 for 22-23 min, 23.1 to 24 min from 50/50 to 100/0, and equilibration at 100/0 for 24-25 min. A flow rate of 0.8 mL min^{-1} was maintained, and absorption was monitored at 265, and 280 nm using commercially available standards for reference, except for the which were chemically synthesized as part of this paper (see below). The column temperature was held at 30 °C.

HPLC Method 3: Detection of Trans cinnamic acid (3a), 3-(4-Hydroxy-3 methoxyphenyl) propionic acid (5a) their aldehyde and amine forms

RP-HPLC system and the column employed were identical to the previously described with a slight variation in the HPLC method. For these chemistries, gradient elution was performed (A/B) with a very shallow gradient from 100/0 to 90/10 for 0-10 min, gradient from 90/10 to 70/30 for 10-16 min, a gradient from 70/30 to 50/50 for 17-19 min, maintenance at 50/50 for 19-22 min, a gradient from 50/50 to 100/0 for 22.1-24 min, and equilibration at 100/0 for 24-25 min. A flow rate of 0.8 mL min^{-1} was maintained, and absorption was monitored at 265, and 280 nm using commercially available standards for reference, except for the which were chemically synthesized as part of this paper (see below). The column temperature was held at 30 °C.

Result and Discussion

***In vitro* screen of CARs for activity on potential lignin-derived carboxylic acids**

We first sought to investigate the specificity of natural CAR homologs on a representative set of lignin-derived carboxylic acids, including vanillate (1a), syringate (2a), trans-cinnamic acid (3a), 3-hydroxy-4-methoxy-trans cinnamic acid (4a), 3-(4-hydroxy-3-methoxyphenyl) propanoic acid (5a) (**Figure 1a**). Here, we chose to focus on 6 CAR homologs based on our recent investigation of CAR specificity on PET deconstruction products (Gopal et al., 2023). Three are

of bacterial origin - srCAR (from *Segniliparus rotundus*) (Duan et al., 2015), maCAR (from *Mycobacterium avium*) (Bayer et al., 2022; Khusnutdinova et al., 2017), mmCAR (from *Mycobacterium marinum*) (Kalim Akhtara et al., 2013; Khusnutdinova et al., 2017) while the other three are of fungal origin - trCAR (from *Trichoderma reesei*) (Gopal et al., 2023; kalbet al., 2014), ncCAR (from *Neurospora crassa*) (Lee et al., 2022; Schwendenwein et al., 2016), afCAR (from *Aspergillus fumigatus*) (Gopal et al.,2023) (**Table S2**). Two of these (trCAR and afCAR) were characterized in our lab for the first time. All the CARs were cloned along with an N-terminal His tag in a pZE vector containing an enzyme for activation of apo-CAR, the 4'-phosphopantetheine transferase encoded by the *sfp* gene from *Bacillus subtilis* (Quadri et al., 1998).

To evaluate substrate specificity and relative activity under defined conditions, we purified all 6 CARs using Ni-affinity chromatography from BL21 DE3 cells expressing holo-CAR. As several of these chemistries absorb light in the same wavelength as NADPH (340 nm), we could not use the traditional plate reader measurement of NADPH depletion and instead measured substrate depletion using reverse phase high performance liquid chromatography (RP-HPLC). To evaluate substrate reduction, we supplied 5 mM of each carboxylic acid in a reaction mixture containing $MgCl_2$, NADPH, ATP, CAR, and ecPPase. We chose an endpoint of 24 h to monitor conversion of 1a-5a. We were encouraged to see that multiple CAR homologs - afCAR, trCAR, and srCAR - exhibited robust activity towards all these substrates **(Figure 2a)**. However, for a given application, one may be interested in CARs that exhibit the fastest conversion of a specific chemistry and the knowledge of which chemistries are most amenable to CARs. Under our conditions, trCAR was the most active among many highly active homologs for 1a, srCAR the most active for 2a (which some fungal CARs did not exhibit as high activity on), mavCAR the most active for 3a, and trCAR the most active for 4a and 5a (for which no CAR exhibited >90%

conversion). If we focus on unique chemical attributes, we observed that unsaturated carboxylic acid side chains are well accepted by the CARs derived from Mycobacterium, that the guaiacol and syringol units are accepted readily by the bacterial CARs tested here, and that longer carboxylate sidechains are accepted by most of these CARs. These results reveal the preferences of CARs towards different kinds of modifications that are characteristic to lignin deconstruction products, and encouragingly most CARs are able to accept most candidate substrates. As such, these reactions produced several aldehydes that are valuable in their own right, with properties relevant for the food and pharmaceutical industries(Kunjapur and Prather, 2015): syringaldehyde (2b) (Lee et al., 2022), cinnamaldehyde (3b) (Ranasinghe et al., 2013; Rao and Gan, 2014), 4-hydroxy-3-methoxy-cinnamaldehyde (4b) (Akber et al., 2015; Thirunavukkarasu et al., 2018), and 3-(4-Hydroxy-3-methoxyphenyl) propanal (5b)(Choi et al., 2017; Kim et al., 2015).

In vitro screen of TAs for activity on potential lignin-derived aldehydes

Given our ability to access diverse aldehydes using CARs and considering many aldehydes are directly derived from lignin without need for the associated carboxylic acid, we next sought to identify enzymes that could generate amines from these aldehydes. We evaluated a small number of members from the transaminase enzyme family (TA, EC 2.6.1) using the ω-TA from *Chromobacter violaceum* (cvTA, WP_011135573) as a starting point (Kaulmann et al., 2007; Yuan et al., 2022). We cloned three TAs (detailed in **Table S1**), including cvTA, *Vibrio fluvialis* (vfTA), and a putative aminotransferase from *Xanthomonas translucens* (xtTA), with N-terminal His-tags for expression in *E. coli*. By using SDS-PAGE and a Western blot on the cell lysates obtained from high cell density expression, we observed soluble expression of all the TAs (**Figure S1**). After expression and purification, we investigated their substrate specificity on commercially available 1b-5b. We carried out the reaction in 0.1 M HEPES (pH 7.5) containing a 4x molar

excess of *i*Pr-NH_2 relative to substrate. As shown in the heatmap (**Figure 2b**), 1b-5b were all efficiently converted to their corresponding amines by the cvTA and vfTA (though vfTA showed lower yield for 3c). Of this small set, we found that cvTA was the most active and broadly specific TA variant. The cvTA and vfTA both exhibit broad substrate specificity, while xtTA has more specific substrate specificity as it showed preference towards 5b. We demonstrated successful formation of primary amines not previously reported including 2c, 4c, and 5c (Fu et al., 2021; Yuan et al., 2023).

Bioconversion of 1a to 1b and 1b to 1c via various formats of biocatalysts

We next sought to compare how the format of this enzyme cascade would affect the observed yields of a model amine product. We evaluated the use of purified enzymes, cell lysates, resting whole cell biocatalysts, and cells growing under aerobic fermentation. The theoretical advantages of using purified enzymes are the abilities to define enzyme concentrations, to exclude competing or inhibitory metabolites, to exclude competing pathways, to avoid potential transport limitations, and to increase storage duration (Hodgman and Jewett, 2012). In contrast, the theoretical advantages of resting whole cells (**Figure 3a-b**) are their abilities to bypass steps of cell lysis and enzyme purification while retaining native systems for co-factor regeneration from simple carbon sources (Domach, 2015; Lin and Tao, 2017). We also hypothesized that resting whole cells could be amenable to catalyst reuse and that some enzymatic reactions in this format may exhibit greater substrate tolerance. Cell lysates fall between these options as cell lysis is still required, the complex cellular milieu is still present excluding the cell membrane, and the storage duration is indefinite upon lyophilization. Finally, we expected that growing cell cultures would be less logical to use for this pathway as its length and orthogonality to native cellular metabolism

would make it unnecessary to add desired substrates during biomass accumulation rather than after, and accumulation of aldehyde intermediates could inhibit growth.

To understand these tradeoffs better for our system, we first investigated the performance of each enzyme individually using the transformation of 1a-1b by srCAR and subsequently the transformation of 1b-1c using cvTA, in all cases examining the reaction yields after 24 h. For the conversion of 1a to 1b using 0.2 mg/mL purified srCAR, we observed complete conversion of 1a to 1b up to 20 mM substrate loading **(Figure S2a)**. When we tested cell lysates that roughly corresponded to 100 mg/mL wet cell weight (wcw), the reaction performed poorly even at low concentrations of provided substrate, resulting in only 23% reaction yield (1.2 mM 1b from 5 mM 1a) **(Figure S2b).** To assess resting whole-cell biocatalysis, we prepared 100 mg/mL wet cell weight (wcw) reaction mix and tested the impact of glucose supplementation for NADPH and ATP co-factor regeneration. Notably, the supplementation of glucose to the resting cells significantly enhanced the conversion from 1a to 1b, demonstrating complete conversion to 1b at a concentration of 20 mM 1a (**Figure 3c**). In contrast, resting cells without glucose supplementation exhibited significantly poor yield, with only 0.57 mM of 1b formed even at a substrate concentration as low as 5 mM (**Figure S2c**). This highlights the crucial role of glucose in facilitating the generation of NADPH and ATP, which are essential for CAR activity.

Given that we obtained good yield using resting whole cells supplemented with glucose, we examined the effect of a higher substrate loading of 50 mM 1a on reaction yield. We observed a vanillin yield of 73.9 ± 10.0 % with a titer of 33.95 ± 4.58 mM of 1b (**Figure 3c)**. In contrast, achieving the same titer in a purified enzyme assay proved unattainable due to the inhibition of srCAR at such high substrate concentrations (as illustrated in **Figure S2a**). Specifically, at 50 mM loading 1a substrate loading, the *in vitro* reaction only yielded a titer of 5 mM for product 1b.

Additionally, from an economic perspective, it is not feasible to use proportional amounts of ATP and NADPH in an *in vitro* system, and alternatively, the purification of co-factor regeneration enzymes also introduces additional cost and labor. Given the efficient carboxylic acid reduction catalyzed by resting whole cells (WC1), we next examined the reaction kinetics on an hourly time scale starting from 5 mM 1a **(Figure 3d).** Under these conditions, we noticed that the reaction was completed within 2 h. Given the speed of this reaction as well as the higher density of cells relative to the solution, we sought to ascertain whether whole cell catalysts could be recycled for the transformation of fresh substrate. Encouragingly, the WC1 whole cells demonstrated nearly complete conversion of 5 mM 1a supplied during all four sequential 2 h batch reactions, with the final round still resulting in >90% yield (**Figure 3e**). The amenability of resting whole cells for catalyst recycling highlights an underexplored advantage of this format that could offer an alternative to traditional enzyme immobilization in batch or flow reactors.

Next, we evaluated the reversible transformation of 1b to 1c catalyzed by cvTA to compare reaction format and conditions, starting with the choice of amine donor. We screened four reported amine donors, including: (i) o-xylylene diamine (o-xyl), which precipitates after amine transfer to shift reaction equilibrium and provide a colorimetric output (Baud et al., 2015; Green et al., 2014); (ii) *i*Pr-NH_2, which is highly volatile and easily recoverable after amine transfer, making it industrially relevant (Dawood et al., 2018; Kelefiotis-Stratidakis et al., 2019; Slabu et al., 2017); (iii) methyl benzylamine (α-MBA), which allows for facile detection of spent amine donor by HPLC-UV(Baud et al., 2015); and, (iv) alanine, which is biosynthetically relevant and offers potential for direct utilization of NH_4^+ after coupling to the alanine dehydrogenase enzyme (Kelefiotis-Stratidakis et al., 2019). Under the conditions that we tested *in vitro*, we found that *i*Pr-NH_2 and α-MBA in 4x excess were the best performing amine donors (**Figure S2d**). We chose to

proceed with *i*Pr-NH_2 in the case of whole cell biocatalysis and briefly investigated cell density and buffer composition to determine if yield could be improved (**Figure S2e**). Surprisingly, when using KP buffer, an unexpected increase in oxidation and over-reduction of vanillin was observed, even while employing the *E. coli* ROAR strain. Ultimately, the most favorable condition tested involved utilizing WC2 cell density of 50 mg/mL (wcw) in 0.1 M HEPES buffer. Using these particular conditions, we obtained a yield of 80.5±0.03% of 1c at our endpoint of 24 h (**Figure 3f**).

Analogous to our approach to characterizing CAR reactions, we next examined the TA reaction kinetics. We found that reaction yield reached 73% after 4 h, remained stagnant at 79% until the mark of 6 h, and then began to gradually unveil the reversible nature of the catalytic reaction facilitated by the TA (**Figure 3g**). We also observed some oxidation and over-reduction of the aldehyde 1b during the later stages of this time course despite using the *E. coli* ROAR expression host. Given the timing of the efficient yield, we next investigated catalyst reusability using two sequential 4 h batches. We observed efficient reaction yields for amine transfer in both these sequential batches, indicating the potential for efficient reusability of the WC2 biocatalyst (**Figure 3h**).

Construction and optimization of one-pot whole cell cascades for 1a to 1c bioconversion

Having shown the ability to successfully use CAR and TA enzymes in both purified enzyme and resting whole cell biocatalytic contexts, we next wanted to investigate how the two transformations could be combined in one pot under the different formats. We sought to test whether the expression of the CAR and TA enzymes in the same cell or in different cells would perform better and how this would compare to the combination of purified enzymes (**Figure 4a**). When we supplied 5 mM 1a to purified enzymes grouped together, we observed a titer of 4.5 ± 0.1 mM of the desired compound 1c (**Figure 4b**). To evaluate whole-cell biocatalysis, we combined

WC1 (100 mg/mL), which overexpressed srCAR, with WC2 (50 mg/mL), which overexpressed cvTA (as listed in **Table S1**). The cells were incubated in a reaction mix supplemented with 110 mM glucose for the biotransformation of 5 mM of 1a to 1c. However, HPLC analysis of the reaction mix collected after 24 h revealed a low yield of 9.6 %, corresponding to 0.54 ± 0.04 mM of 1c, while a substantial portion (87.4%) of the intermediate compound 1b was formed, amounting to 4.8 ± 0.1 mM (**Figure 4b**). This suggested that the reaction catalyzed by the cvTA was the bottleneck in resting whole cells.

As a first step towards understanding underlying factors causing cvTA whole cells (WC2) activity stalling on 1b, we tested the combination of srCAR whole cells and purified cvTA in one pot. However, we discovered that TA activity remains restricted under these conditions and that the whole cells generate a product that inhibits the desired amine transfer reaction. Notably, the only variable was the addition of glucose, which plays an important role in regenerating co-factors needed by CAR through the action of intracellular enzymes (Napora-Wijata et al., 2014). However, glucose metabolism in resting whole cell biocatalysts generates substantial amounts of alternative amine acceptors such as pyruvate (Sarak et al., 2022). Our experiments showed that cvTA activity is indeed hindered in the presence of higher glucose concentrations (**Figure S3a**), however, we were able to identify a specific glucose concentration that significantly improved 1c yield in the one pot condition (**Figure S3b**). To further understand the glucose concentration requirements, we quantified glucose consumption by HPLC and saw that approximately 10 mM was consumed during the biotransformation of 5 mM 1a (**Figure S3c**). Based on related literature on TA bioconversions using whole cells (Fedorchuk et al., 2020; Truppo et al., 2009), we sought to compare this approach to an alternative solution of co-expressing alanine dehydrogenase (AlaDH), which consumes pyruvate and NH_4^+ to form the amine donor alanine (**Figure S3d**). We prepared

WC3 cells which harbor AlaDH from *B. subtilis* in the pACYC plasmid along with cvTA. We compared the one pot assay for 1a to 1c utilizing either WC1+WC2 cells or WC1+WC3 cells when supplemented with 10 mM of glucose at 5 mM substrate loading and observed equivalent yields (**Figure 4c**).

To explore whether reaction yield could improve further by consolidating the CAR and TA enzymes into one host, we prepared WC4 cells (**Figure 4a**) which harbor pZE-srCAR-sfp and pACYC-cvTA-AlaDH. In these cells, we found that CAR activity was limited (**Figure 4d**), which could be attributed to lower expression levels of CAR vs Sfp due to translational resource burden (**Figure S4**). In particular, the high strength T7 promoter used for TA and AlaDH expression could potentially outcompete the pTet promoter used for CAR and Sfp expression (Deich et al., 2023). To address this, we subcloned CAR and Sfp so that they would each be under a separate T7 promoter rather than in one operon (WC5: **Figure 4a**). This approach resulted in a substantial 9.1-fold enhancement in the yield of 1c compared to WC4 settings (**Figure 4d**). We further examined the effect of IPTG concentration (ranging from 0.1 to 1 mM) on the expression of all four enzymes in WC5 cells under P1 expression conditions. Using SDS-PAGE and Western analysis, we found that an IPTG concentration of 0.75 mM yielded optimal expression levels for all four enzymes (**Figure S5**). To evaluate the potential role of AlaDH in altering the equilibrium of the transaminase-catalyzed reaction by recycling pyruvate (Slabu et al., 2017; Truppo et al., 2009), we conducted experiments using WC5 cells under varying glucose concentrations. Under normal circumstances, the WC5 cells exhibited negligible transaminase activity on 1b at approximately 50 mM glucose (**Figure S3a&b**). However, when the AlaDH was present and expressed, the whole cells demonstrated an enhanced capacity to tolerate higher glucose concentration (**Figure S3e**), beyond the 50 mM glucose threshold where the cvTA typically exhibited minimal activity.

Examining WC5 whole cell biocatalyst substrate tolerance, reusability, and harvesting

We next investigated the substrate tolerance towards 1a and the reaction yield using the optimized conditions for whole cell biocatalysis. Since increases in substrate loading must be accompanied by increases in amine donor concentration or spent amine recycling, we first investigated the influence of *i*Pr-NH_2 concentration on reaction yield and found we could go as high as 40 mM without loss of yield and biproduct formation (**Figure S6**). Therefore, for substrate tolerance experiments, we chose to limit the maximum *i*Pr-NH_2 concentration to 40 mM. We observed near complete conversion of 1a to 1c up to 10 mM substrate loading. Furthermore, at a substrate loading of 20 mM 1a, a yield of 67.29% 1c was achieved with a whole cell loading of 100 mg/mL within a 24 h timeframe **(Figure 5a).** Interestingly, we observed that supplementing an additional 100 mg/mL of whole cells 6 h after reaction initiation led to further improvement in the reaction yield to 80.9% for 20 mM substrate loading (**Figure 5a**). These findings suggest the potential of this catalyst for handling higher substrate concentrations while maintaining significant yields.

In our recent study, we presented evidence showcasing the substantial influence of the duration of culturing prior to harvesting resting cell biocatalysts on aldehyde stability (Butler et al., 2023). Having demonstrated biocatalyst reusability for each step individually, we next examined the reusability of WC5 by harvesting fresh batches under both P1 (longer culture duration) and P2 expression conditions (shorter culture duration) (see footnote in **Table S2**). In this case, cells were either immediately used or stored for only 24 h prior to resting cell assay. Given that we had seen near to complete conversion of 1a to 1c within 6 h at 5 mM substrate loading (**Figure 5a**), we decided to perform 6 h batch reactions for whole cell reusability. We reused recovered WC5 for a total of 4 reaction cycles. We observed that WC5 cells harvested using

P2 expression conditions could be reused up to three times without a significant reduction in productivity. Our findings indicate that delaying the harvesting of cells (longer culture duration) resulted in decreased efficiency. The yield obtained from cells harvested using P1 conditions was 36.8%, while cells harvested using P2 conditions showed a higher yield of 55.4% at the end of the 3rd round. By the end of the 4th round, we observed that the cells were beginning to show poor efficiency. To understand whether these poor conversion rates were associated with slow reaction kinetics, we extended the sampling period to 24 h (**Figure 5b**). It was observed that the whole cell harvested using the P2 expression condition (shorter culture duration), their reusability could even be extended to the fourth round, with a remarkable yield of 71.2% compared to a mere 27.43% yield observed in P1 harvested cells at 24 hours. These results highlight the importance of optimizing the duration of culturing and harvesting conditions to maximize productivity and yield in whole-cell biocatalysis experiments, and further confirms that whole cells remain robust and catalytically active for 1c production during repetitive use.

Whole-cell biocatalysis for one-pot synthesis of other aryl primary amines (2c-5c)

Having thoroughly optimized the whole-cell system for low-cost and efficient conversion of 1a-1c, we finally tested the ability of WC5 cells to convert our original panel of carboxylic acids (2a-5a) to their corresponding amines (2c-5c). The HPLC results indicate that nearly complete conversion was obtained of acids to amines for most substrates, except 2a. Interestingly, the CAR enzyme appeared to be a bottleneck specifically at whole cell level (**Figure 6a**), as complete conversion to 2c was achieved using the same enzyme cascade in an *in vitro* setting, this suggests further investigation opportunities would be valuable to enhance the yield, potentially by optimizing the cellular environment and enzyme selection (Lee et al., 2022). In contrast, 3a, 4a and 5a bioconversions were highly efficient reaching equal or more than 90% substrate depletion,

producing the desired 3c, 4c and 5c product with no detectable byproducts within 6 h (**Figure 6b-d)**. The HPLC traces displayed a higher product yield at both 6 h and 24 h, with peak retention matching to the *in vitro* assay traces, and no matching peaks were observed in the control. Notably, 3c yield was observed to be much higher at 6 h time point compared to 24 h, indicated by peak areas, at 24 h timepoint the reaction appeared to be affected by equilibrium dynamics and a minor 3a peak was observed. The results highlight the potential of our method in expanding the scope of amine synthesis and provide valuable insights for future developments in this field.

Discussion

In this work, we sought to develop a cost-effective and operationally simple method for the selective synthesis of a variety of aromatic aldehydes and primary amines from lignin-derived carboxylic acids (1a-5a). To achieve this, we designed a one pot biocatalytic transformation that is informed by the substrate specificity of diverse CARs and TAs. In recent times, there has been a growing interest among researchers in investigating the potential of CARs and TAs for diverse chemistries and applications (Citoler et al., 2019; Duan et al., 2015; France et al., 2016; Gopal et al., 2023; Kalim Akhtara et al., 2013). Leveraging the new substrate specificity information gained from our study, we have conducted a detailed characterization of two important reaction formats, namely cell-free biocatalysis and resting whole-cell biocatalysis. This allowed us to explore and improve the performance of resting whole cell biocatalysts which offer some practical advantages offers over the use of fermentation or purified enzymes. These advantages include easy catalyst separation, elimination of cell lysis and enzyme purification steps, and the ability to better tolerate conditions that are inhibitory to cell growth or purified enzymes (Doyon et al., 2022; Hepworth et al., 2017). Purified enzymes offer theoretical advantages such as precise control over enzyme concentrations and exclusion of competing metabolites and pathways, however, their use often

requires expensive cofactors to sustain optimal enzyme activity. In contrast, resting whole cells utilize native systems for co-factor regeneration from simple carbon sources. We have also explored cell lysates very briefly, which fall between these options, requiring cell lysis but retaining the complex cellular milieu. However, the reaction yields were significantly poor for this instance. Furthermore, using fermentation may not be as preferable for this pathway due to the orthogonality of the pathway to native cellular metabolism and the presence of chemistries that could inhibit growth.

Having shown the ability to successfully use CAR and TA enzymes in both purified enzyme and resting whole cell biocatalytic contexts, we next wanted to investigate how the two transformations could be combined in one pot under the different formats. We also compared performance of the whole cells with the purified enzymes when added together to a common reaction medium. When opting for whole cells, we noticed that the TA-catalyzed reaction stalled. We observed that higher glucose supplementation, which was intended for cofactor regeneration, had a deleterious impact on the biocatalytic system. This indicates some need for considering an optimal glucose concentration that promotes the ATP and NADPH regeneration necessary for CAR (Yuan et al., 2022) and the need to consider consumption of native alternative amine acceptors. The expression of AlaDH can regenerate the amine donor alanine while depleting metabolically produced pyruvate, which appears to allow a higher initial glucose concentration. We next tested whether the expression of the CAR and TA enzymes in the same cell or in different cells would perform better under different cloning strategies. Our results demonstrate that resting whole-cell reactions can be highly competitive with cell-free reactions, yielding 97% and 70% conversion rates, respectively at 5 mM substrate loading. Given the efficient yield observed at 5 mM substrate loading, we aimed to investigate substrate tolerance and reusability of the final clone

WC5. Additionally, building upon the knowledge gained from this study, we have expanded the scope of our investigation to produce several amines from carboxylic acid precursors using one-pot biocatalytic reactions. We achieved the synthesis of various amines, including compounds 1c-5c.

The outcomes of our work represent an advancement in the utilization of both cell-free and cell-based approaches to incorporate amine functionality into lignin-derived building blocks. The intermediate aldehyde compounds synthesized in this study, such as (1b-5b), exhibit a wide range of bioactive properties having promising potential in various applications including the development of therapeutic agents, natural preservatives, flavor enhancers, and biobased plasticizer (Fache et al., 2014; Kim et al., 2015; Lee et al., 2022; Ranasinghe et al., 2013; Su et al., 2022). By leveraging the capabilities of threonine aldolases, threonine trans-aldolases, and transaminases enzyme classes and utilizing the currently synthesized aromatic aldehydes as substrates or intermediates, researchers can expand the scope of other biosynthetic processes that harness aldehyde intermediates, such as non-standard amino acids (Doyon et al., 2022; Slabu et al., 2017; Song et al., 2018). Herein, we have employed an engineered *E. coli* strain that exhibits lower endogenous rates of aldehyde oxidation and reduction to facilitate resting cell biocatalysis. Particularly for chemistries that feature toxic products or intermediates such as aldehydes, resting cells offer a compelling biocatalytic format (Butler et al., 2023).

The aryl primary amines synthesized in this study hold potential value for diverse applications. One such application is carbon capture, where aryl primary amines can be utilized as sorbents for the efficient capture and separation of carbon dioxide (CO_2). The development of solid sorbents with amine-containing side chains offers advantages such as improved stability, reduced energy requirements, and enhanced recyclability compared to conventional liquid amine systems

(Hallenbeck and Kitchin, 2013). Moreover, homo and cross coupling between these aryl amines could lead to more complex molecular structures for the development of advanced polymers (Mohamad et al., 2010; Sahu et al., 2010). A recent study on one-pot polymerization of aryl dihalides with primary aryl amines reported the formation of highly efficient solution processable polymers for Perovskite Solar Cells (Astridge et al., 2021). Notably, the application of cinnamylamine in the synthesis of naftifine, an effective antifungal medication, exemplifies the ability of aryl primary amines to be used as building blocks for therapeutics (Yuan et al., 2023). In conclusion, the extensive utilization of aryl primary amines across industries such as pharmaceuticals, polymers, pesticides, dyes, and detergents underscore their importance as key building blocks in the chemical industry.

Conclusion

In this work, we synthesized structurally diverse aldehydes and amines from lignin deconstruction products using multiple biocatalytic formats to expand the repertoire of chemicals that can be obtained from waste biomass. Our objectives were to create enzyme cascades for converting lignin derivable carboxylic acids into amines, to determine their substrate specificity, to optimize the performance of a potential resting whole cell biocatalyst, and to evaluate the ability to reuse the whole cell biocatalyst. We believe similar kinds of enzymatic transformation routes will be applicable to other lignin-derived substrates, such as those that are pre-functionalized for polymerization (Nain et al., 2023 ("in preparation")). Overall, our work generates new knowledge and tools for the design of chemical syntheses from sustainable sources that could benefit diverse industries.

Abbreviations: CAR, carboxylic acid reductase; ω-TA, ω-transaminase; NADPH, nicotinamide adenine dinucleotide phosphate (reduced); ATP, adenosine5′-triphosphate; *i*Pr-NH_2, isopropyl amine; α-MBA, methylbenzyl amine; wcw, wet cell weight.

Author Statement: A.M.K. conceived the study, secured funding, supervised the study, and helped write the manuscript; P.N. designed and conducted all the experiments, analyzed data, prepared figures, and wrote most of the manuscript; R.M.D. cloned the AlaDH gene; V.S. assisted with substrate tolerance and WC5 reusability experiment; M.S. performed preliminary experiments.

Acknowledgments: We acknowledge the support from the National Science Foundation (NSF GCR CMMI-1934887). The cloning work was conducted as part of proposal 506446 at the U.S. Department of Energy Joint Genome Institute, DOE science user facility, supported by the Office of Science of the U.S. Department of Energy, operating under contract no. DE-AC02-05CH11231. We thank the Mass Spectrometry Facility at the University of Delaware for the mass spectrometry analysis that is supported by the National Institute of General Medical Sciences of the National Institutes of Health under award P20GM104316 and Katherine Martin in particular for her assistance.

Declaration of Competing Interest: The authors declare the following competing financial interest(s): A.M.K., P.N., and R.M.D. have filed for a provisional patent related to CAR and TA cascades. The remaining authors declare no competing interest.

References

Abdel-Magid AF, Carson KG, Harris BD, Maryanoff CA, Shah RD. 1996. Reductive Amination of Aldehydes and Ketones with Sodium Triacetoxyborohydride. Studies on Direct and Indirect Reductive Amination Procedures 1. *Journal of organic chemistry* **61**:3849–3862.

Akber U, Na BR, Ko YS, Lee HS, Kim HR, Kwon MS, Park ZY, Choi EJ, Han WC, Lee SH, Oh HM, Jun CD. 2015. Phytocomponent 4-hydroxy-3-methoxycinnamaldehyde ablates T-cell activation by targeting protein kinase C-θ and its downstream pathways. *Int Immunopharmacol* **25**:130–140.

Astridge DD, Hoffman JB, Zhang F, Park SY, Zhu K, Sellinger A. 2021. Polymer Hole Transport Materials for Perovskite Solar Cells via Buchwald-Hartwig Amination. *ACS Appl Polym Mater* **3**:5578–5587.

Baud D, Ladkau N, Moody TS, Ward JM, Hailes HC. 2015. A rapid, sensitive colorimetric assay for the high-throughput screening of transaminases in liquid or solid-phase. *Chemical Communications* **51**:17225–17228.

Bayer T, Pfaff L, Branson Y, Becker A, Wu S, Bornscheuer UT, Wei R. 2022. Biosensor and chemo-enzymatic one-pot cascade applications to detect and transform PET-derived terephthalic acid in living cells. *iScience* **25**.

Butler ND, Anderson SR, Dickey RM, Nain P, Kunjapur AM. 2023. Combinatorial gene inactivation of aldehyde dehydrogenases mitigates aldehyde oxidation catalyzed by E. coli resting cells. *Metab Eng* **77**:294–305.

Butler N, Kunjapur AM. 2020. Carboxylic acid reductases in metabolic engineering. *J Biotechnol* **307**:1–14.

Choi SK, Mun GI, Choi E, Kim SY, Kwon Y, Na Y, Lee YS. 2017. The Conjugated Double Bond of Coniferyl Aldehyde Is Essential for Heat Shock Factor 1 Mediated Cytotoprotection. *J Nat Prod* **80**:2379–2383.

Citoler J, Derrington RS, Galman J, Bevinakatti H, Turner N. 2019. A biocatalytic cascade for the conversion of fatty acids to fatty amines. *Green Chemistry* **21**.

Cui Y, Goes SL, Stahl SS. 2021. Sequential oxidation-depolymerization strategies for lignin conversion to low molecular weight aromatic chemicals. *Adv Inorg Chem*. Academic Press Inc., Vol. 77, pp. 99–136.

Dawood AWH, Weiß MS, Schulz C, Pavlidis I V., Iding H, de Souza ROMA, Bornscheuer UT. 2018. Isopropylamine as Amine Donor in Transaminase-Catalyzed Reactions: Better Acceptance through Reaction and Enzyme Engineering. *ChemCatChem* **10**:3943–3949.

Deich C, Cash B, Sato W, Sharon J, Aufdembrink L, Gaut NJ, Heili J, Stokes K, Engelhart AE, Adamala KP. 2023. T7Max transcription system. *J Biol Eng* **17**:1–14.

Dhers S, Vantomme G, Avérous L. 2019. A fully bio-based polyimine vitrimer derived from fructose. *Green Chemistry* **21**:1596–1601.

Domach MM. 2015. Perspectives and Prospects for Whole Cell Catalysis. *Catal Letters* **145**:346–359.

Doyon TJ, Kumar P, Thein S, Kim M, Stitgen A, Grieger AM, Madigan C, Willoughby PH, Buller AR. 2022. Scalable and Selective β-Hydroxy-α-Amino Acid Synthesis Catalyzed by Promiscuous l-Threonine Transaldolase ObiH. *ChemBioChem* **23**:1–9.

Duan Y, Yao P, Chen X, Liu X, Zhang R, Feng J, Wu Q, Zhu D. 2015. Exploring the synthetic applicability of a new carboxylic acid reductase from Segniliparus rotundus DSM 44985. *J Mol Catal B Enzym* **115**:1–7.

Fache M, Boutevin B, Caillol S. 2016. Vanillin Production from Lignin and Its Use as a Renewable Chemical. *ACS Sustain Chem Eng* **4**:35–46.

Fache M, Darroman E, Besse V, Auvergne R, Caillol S, Boutevin B. 2014. Vanillin, a promising biobased building-block for monomer synthesis. *Green Chemistry* **16**:1987–1998.

Fedorchuk TP, Khusnutdinova AN, Evdokimova E, Flick R, Leo R Di, Stogios P, Savchenko A, Yakunin AF. 2020. One-Pot Biocatalytic Transformation of Adipic Acid to 6 - Aminocaproic Acid and 1,6-Hexamethylenediamine Using Carboxylic Acid Reductases and Transaminases. *J Am Chem Soc* **142**:1038–1048.

France SP, Hussain S, Hill AM, Hepworth LJ, Howard M, Mulholland KR, Flitsch SL, Turner NJ. 2016. One Pot Cascade Synthesis of Mono- and Di- Substituted Piperidines and Pyrrolidines using Carboxylic Acid Reductase (CAR), ω -Transaminase (ω -TA), and Imine Reductase (IRED) Biocatalysts. *ACS Catal* **6**:3753–3759.

Fu B, Xiao G, Zhu Y, Chen Y, Lai Y, Yuan J. 2021. Renewable Vanillylamine Synthesis from Lignin-Derived Feedstocks. *ACS Agricultural Science and Technology* **1**:566–571.

Gopal MR, Dickey RM, Butler ND, Talley MR, Nakamura DT, Mohapatra A, Watson MP, Chen W, Kunjapur AM. 2023. Reductive Enzyme Cascades for Valorization of Polyethylene Terephthalate Deconstruction Products. *ACS Catal* **13**:4778–4789.

Green AP, Turner NJ, O'Reilly E. 2014. Chiral amine synthesis using ω-transaminases: An amine donor that displaces equilibria and enables high-throughput screening. *Angewandte Chemie - International Edition* **53**:10714–10717.

Guggari S, Magliozzi F, Malburet S, Graillot A, Destarac M, Guerre M. 2023. Vanillin-Based Epoxy Vitrimers: Looking at the Cystamine Hardener from a Different Perspective. *ACS Sustain Chem Eng* **11**:6021–6031.

Hakkarainen M, Xu Y, Odelius K. 2020. Photocurable, thermally reprocessable, and chemically recyclable vanillin-based imine thermosets. *ACS Sustain Chem Eng* **8**:17272–17279.

Hallenbeck AP, Kitchin JR. 2013. Effects of O2 and SO2 on the capture capacity of a primary-amine based polymeric CO2 sorbent. *Ind Eng Chem Res* **52**:10788–10794.

Hepworth LJ, France SP, Hussain S, Both P, Turner NJ, Flitsch SL. 2017. Enzyme Cascades in Whole Cells for the Synthesis of Chiral Cyclic Amines. *ACS Catal* **7**:2920–2925.

Hodgman CE, Jewett MC. 2012. Cell-free synthetic biology: Thinking outside the cell. *Metab Eng* **14**:261–269.

Höhne M, Bornscheuer UT. 2009. Biocatalytic routes to optically active amines. *ChemCatChem* **1**:42–51.

Holmberg AL, Nguyen NA, Karavolias MG, Reno KH, Wool RP, Epps TH. 2016a. Softwood Lignin-Based Methacrylate Polymers with Tunable Thermal and Viscoelastic Properties. *Macromolecules* **49**:1286–1295.

Holmberg AL, Reno KH, Nguyen NA, Wool RP, Epps TH. 2016b. Syringyl Methacrylate, a Hardwood Lignin-Based Monomer for High-Tg Polymeric Materials. *ACS Macro Lett* **5**:574–578.

José Borges Gomes F, de Souza RE, Brito EO, Costa Lelis RC. 2020. A review on lignin sources and uses. *J. Appl. Biotechnol. Bioeng.* **7**:100–105.

kalb D, Lackner G, Hoffmeister D. 2014. Functional and phylogenetic divergence of fungal adenylate-forming reductases. *Appl Environ Microbiol* **80**:6175–6183.

Kalim Akhtara M, Turner NJ, Jones PR. 2013. Carboxylic acid reductase is a versatile enzyme for the conversion of fatty acids into fuels and chemical commodities. *Proc Natl Acad Sci U S A* **110**:87–92.

Kaulmann U, Smithies K, Smith MEB, Hailes HC, Ward JM. 2007. Substrate spectrum of ω-transaminase from Chromobacterium violaceum DSM30191 and its potential for biocatalysis. *Enzyme Microb Technol* **41**:628–637.

Kelefiotis-Stratidakis P, Tyrikos-Ergas T, Pavlidis I V. 2019. The challenge of using isopropylamine as an amine donor in transaminase catalysed reactions. *Org Biomol Chem* **17**:1634–1642.

Khusnutdinova AN, Flick R, Popovic A, Brown G, Tchigvintsev A, Nocek B, Correia K, Joo JC, Mahadevan R, Yakunin AF. 2017. Exploring Bacterial Carboxylate Reductases for the Reduction of Bifunctional Carboxylic Acids. *Biotechnol J* **12**.

Kim SY, Lee HJ, Nam JW, Seo EK, Lee YS. 2015. Coniferyl aldehyde reduces radiation damage through increased protein stability of heat shock transcriptional factor 1 by phosphorylation. *Int J Radiat Oncol Biol Phys* **91**:807–816.

Kunjapur AM, Cervantes B, Prather KLJ. 2016. Coupling carboxylic acid reductase to inorganic pyrophosphatase enhances cell-free in vitro aldehyde biosynthesis. *Biochem Eng J* **109**:19–27.

Kunjapur AM, Prather KLJ. 2015. Microbial engineering for aldehyde synthesis. *Appl Environ Microbiol* **81**:1892–1901.

Kunjapur AM, Tarasova Y, Prather KLJ. 2014. Synthesis and Accumulation of Aromatic Aldehydes in an Engineered Strain of Escherichia coli. *J Am Chem Soc* **136**:11644–11654.

Lee HS, Park J, Yeon YJ. 2022. Biocatalytic valorization of lignin subunit: Screening a carboxylic acid reductase with high substrate preference to syringyl functional group. *Enzyme Microb Technol* **161**.

Lee J, McGrath AJ, Hawker CJ, Kim BS. 2016. pH-Tunable Thermoresponsive PEO-Based Functional Polymers with Pendant Amine Groups. *ACS Macro Lett* **5**:1391–1396.

Lin B, Tao Y. 2017. Whole-cell biocatalysts by design. *Microb Cell Fact*. BioMed Central Ltd **16**:1-12.

Mohamad D, Johnson RG, Janeliunas D, Kirkus M, Yi H, Lidzey DG, Iraqi A. 2010. Aryl amine substituted low energy gap carbazole polymers: Preparation and photovoltaic properties. *J Mater Chem* **20**:6990–6997.

Molinari F, Pollegioni L, Rosini E. 2023. Whole-Cell Bioconversion of Renewable Biomasses-Related Aromatics to cis,cis-Muconic Acid. *ACS Sustain Chem Eng* **11**:2476–2485.

Napora-Wijata K, Robins K, Osorio-Lozada A, Winkler M. 2014. Whole-cell carboxylate reduction for the synthesis of 3-hydroxytyrosol. *ChemCatChem* **6**:1089–1095.

Nain P, Christoff-Tempesta T, Dickey RG, Epps TH III, & Kunjapur AM. 2023. Enabling Polymerization-Ready Biocatalytic Amine Transfer to Functionalized Lignin-Derived Carboxylic Acids and Aldehydes. Department of Chemical and Biomolecular Engineering, University of Delaware.

Ngo HPT, Nguyen DQ, Park H, Park YS, Kwak K, Kim T, Lee JH, Cho KS, Kang LW. 2022. Conformational change of organic cofactor PLP is essential for catalysis in PLP-dependent enzymes. *BMB Rep* **55**:439–446.

O'Dea RM, Pranda PA, Luo Y, Amitrano A, Ebikade EO, Gottlieb ER, Ajao O, Benali M, Vlachos DG, Ierapetritou M, Epps TH. 2022. Ambient-pressure lignin valorization to high-performance polymers by intensified reductive catalytic deconstruction. *Sci. Adv* **8**:7523.

Podyacheva E, Afanasyev OI, Tsygankov AA, Makarova M, Chusov D. 2019. Hitchhiker's Guide to Reductive Amination. *Synthesis (Germany)* **51**:2667–2677.

Quadri LEN, Weinreb PH, Lei M, Nakano MM, Zuber P, Walsh CT. 1998. Characterization of Sfp, a Bacillus subtilis Phosphopantetheinyl Transferase for Peptidyl Carrier Protein Domains in Peptide Synthetases †. *Biochem* **37**:1585–1595.

Rahimi A, Ulbrich A, Coon JJ, Stahl SS. 2014. Formic-acid-induced depolymerization of oxidized lignin to aromatics. *Nature* **515**:249–252.

Ranasinghe P, Pigera S, Premakumara GS, Galappaththy P, Constantine GR, Katulanda P. 2013. Medicinal properties of "true" cinnamon (Cinnamomum zeylanicum): A systematic review. *BMC Complement Altern Med* **13**.

Rao PV, Gan SH. 2014. Cinnamon: A multifaceted medicinal plant. *Evidence-based Complementary and Alternative Medicine* **2014**.

Rocha JF, Pina AF, Sousa SF, Cerqueira NMFSA. 2019. PLP-dependent enzymes as important biocatalysts for the pharmaceutical, chemical and food industries: A structural and mechanistic perspective. *Catal Sci Technol* **9**:4864–4876.

Sahu D, Padhy H, Patra D, Huang JH, Chu CW, Lin HC. 2010. Synthesis and characterization of novel low-bandgap triphenylamine-based conjugated polymers with main-chain donors and pendent acceptors for organic photovoltaics. *J Polym Sci A Polym Chem* **48**:5812–5823.

Sarak S, Pagar AD, Khobragade TP, Jeon H, Giri P, Lim S, Patil MD, Kim Y, Kim BG, Yun H. 2022. A multienzyme biocatalytic cascade as a route towards the synthesis of α,ω-diamines from corresponding cycloalkanols. *Green Chemistry* **25**:543–549.

Schutyser W, Renders T, Van Den Bosch S, Koelewijn SF, Beckham GT, Sels BF. 2018. Chemicals from lignin: An interplay of lignocellulose fractionation, depolymerisation, and upgrading. *Chem Soc Rev* **47**:852–908.

Schwendenwein D, Fiume G, Weber H, Rudroff F, Winkler M. 2016. Selective Enzymatic Transformation to Aldehydes in vivo by Fungal Carboxylate Reductase from Neurospora crassa. *Adv Synth Catal* **358**:3414–3421.

Slabu I, Galman JL, Lloyd RC, Turner NJ. 2017. Discovery, Engineering, and Synthetic Application of Transaminase Biocatalysts. *ACS Catal* **7**:8263–8284.

Song W, Wang JH, Wu J, Liu J, Chen XL, Liu LM. 2018. Asymmetric assembly of high-value α-functionalized organic acids using a biocatalytic chiral-group-resetting process. *Nat Commun* **9**:1–9.

Su ZM, Twilton J, Hoyt CB, Wang F, Stanley L, Mayes HB, Kang K, Weix DJ, Beckham GT, Stahl SS. 2022. Ni- and Ni/Pd-Catalyzed Reductive Coupling of Lignin-Derived Aromatics to Access Biobased Plasticizers. *ACS Cent Sci* **9**:159–165.

Sun Z, Fridrich B, De Santi A, Elangovan S, Barta K. 2018. Bright Side of Lignin Depolymerization: Toward New Platform Chemicals. *Chem Rev* **118**:614–678.

Thirunavukkarasu K, Rajkumar P, Selvaraj S, Suganya R, Kesavan M, Gunasekaran S, Kumaresan S. 2018. Vibrational (FT-IR and FT-Raman), electronic (UV–Vis), NMR (1H and 13C) spectra and molecular docking analyses of anticancer molecule 4-hydroxy-3-methoxycinnamaldehyde. *J Mol Struct* **1173**:307–320.

Truppo MD, Rozzell JD, Moore JC, Turner NJ. 2009. Rapid screening and scale-up of transaminase catalysed reactions. *Org Biomol Chem* **7**:395–398.

Upton BM, Kasko AM. 2016. Strategies for the conversion of lignin to high-value polymeric materials: Review and perspective. *Chem Rev* **116**:2275–2306.

Wang H, Pu Y, Ragauskas A, Yang B. 2019a. From Lignin to Valuable Products-Strategies, Challenges, and Prospects. *Bioresour. Technol.* **271**:449–461.

Wang S, Shuai L, Saha B, Vlachos DG, Epps TH. 2018b. From Tree to Tape: Direct Synthesis of Pressure Sensitive Adhesives from Depolymerized Raw Lignocellulosic Biomass. *ACS Cent Sci* **4**:701–708.

Yuan S, Jin M, Xu C, Yin W, Zhao M, Xian M, Liu W. 2022. Self-sufficient whole-cell biocatalysis for 3-(aminomethyl) pyridine synthesis. *Biochem Eng J* **183**.

Yuan S, Xu C, Jin M, Xian M, Liu W. 2023. Synergistic improvement of cinnamylamine production by metabolic regulation. *J Biol Eng* **17**.

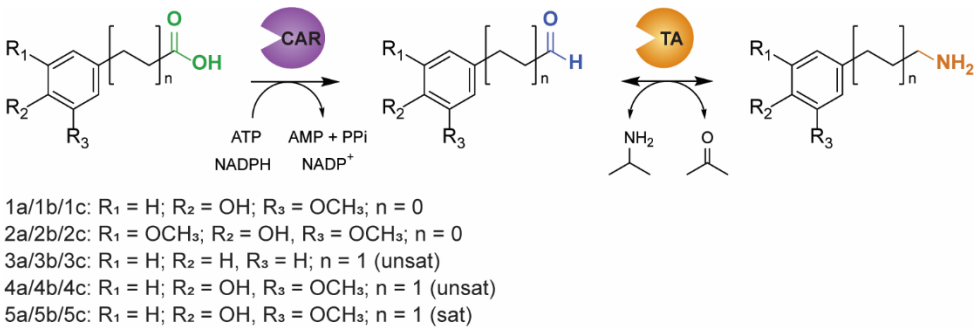

Figure 1. Envisioned transformations catalyzed by enzyme cascades in this study. This schematic shows the envisioned conversion of guaiacol and syringol substituted carboxylic acids and aldehydes to their corresponding amines catalyzed by a carboxylic acid reductase (CAR) and ω-transaminase (TA). We compare two formats for this biocatalytic cascade: purified enzymes or resting whole cells that overexpress cascade enzymes beside substrate specificity.

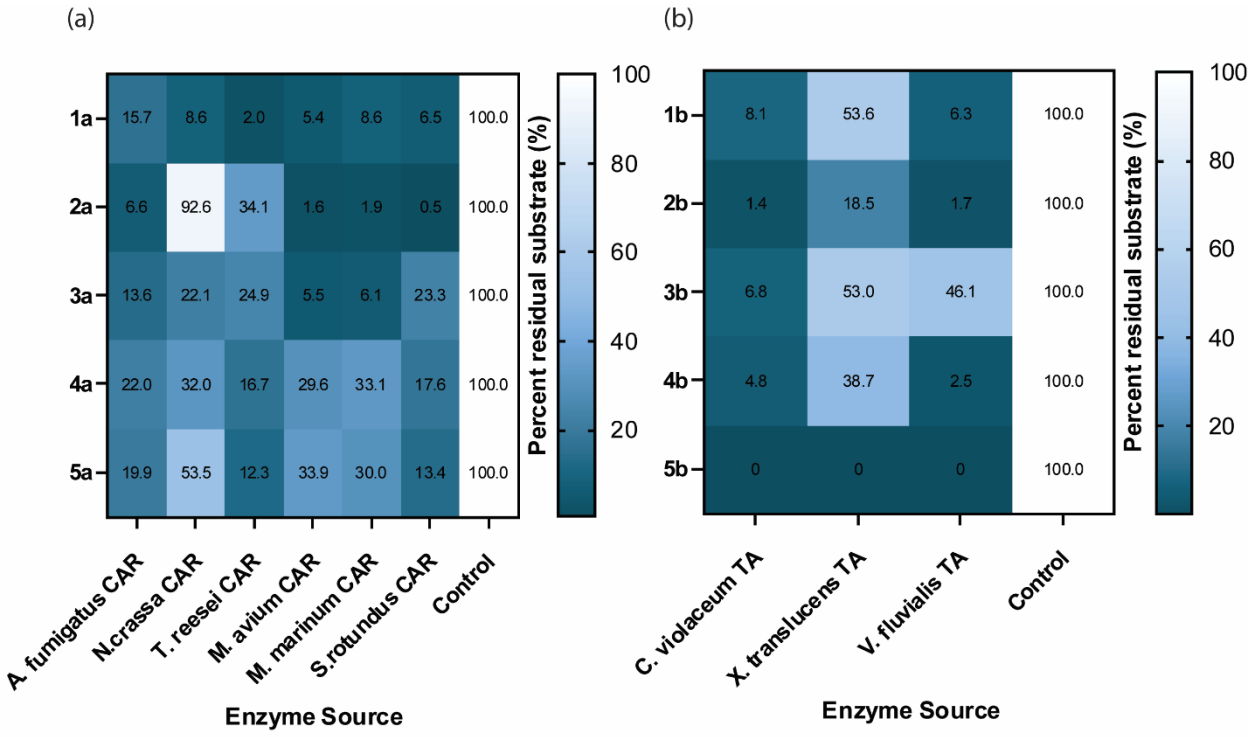

Figure 2. Evaluation of CAR and TA substrate specificity on lignin-derivable small molecules as measured by assays using purified enzymes. (a) Screening of naturally occurring CARs for the production of aryl aldehydes from lignin-derivable aryl carboxylic acids. The results demonstrate the identification of a suitable naturally occurring CAR variant for all chemistries envisioned in

Figure 1. CAR reactions contained 0.2 mg/mL of respective CAR added to 0.1 M HEPES pH 7.5, 10 mM $MgCl_2$, 1x NADPH, and 1.25x ATP. Substrate depletion was measured using RP-HPLC-UV at a desired endpoint of 24 h (except 1 h for 6a and 7a due to hydrolysis). (b) Screening of naturally occurring TAs for the production of aryl amines from aryl aldehydes. TA reactions contained 0.5 mg/mL of respective TA added to 0.1 M HEPES pH 7.5, 2 mM PLP, and 4x *i*Pr-NH_2 as the amine donor. Substrate depletion was measured using RP-HPLC-UV at a desired endpoint of 24 h.

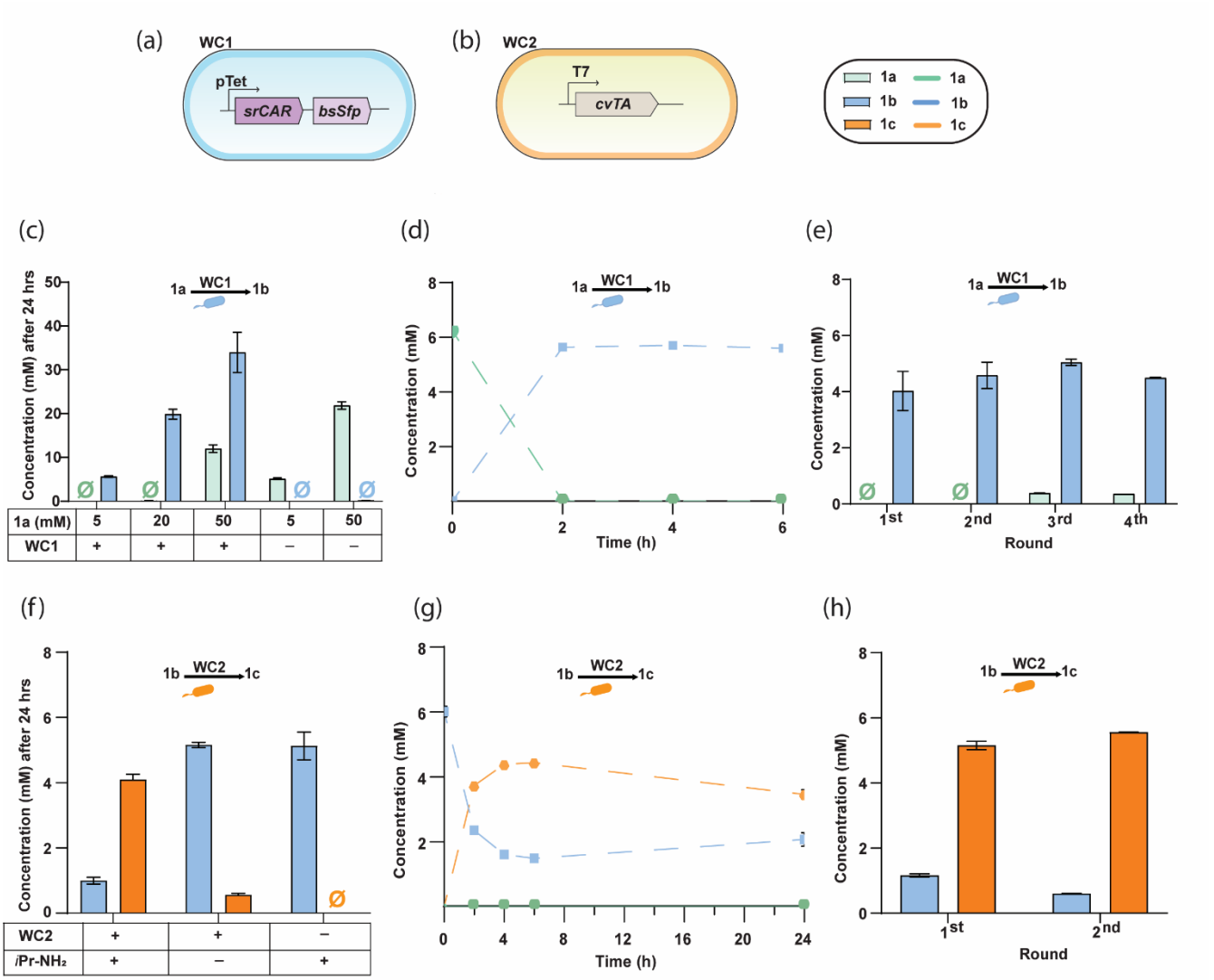

Figure 3. Evaluation of individual transformation steps catalyzed by either srCAR or cvTA expressing whole cells on the model substrates 1a or 1b under fermentative or resting whole cell biocatalyst format (100 mg/mL wet cell weight). (a-b) Illustration of the whole cells expressing

srCAR and cvTA. (c) Endpoint concentrations of 1a and 1b as a function of 1a loading concentration at our chosen time point of 24 h using "WC1" (cells transformed to express srCAR and bsSfp). Resting cells were incubated at 30 °C in 0.1 M HEPES pH 7.5 and 10 mM $MgCl_2$ with 100 mM glucose for cofactor regeneration. (d) Time-course kinetics of the reduction of 1a to 1b catalyzed by WC1 cells, which reached completion within 2 h. (e) Demonstration of WC1 reusability in rounds of batch catalysis initiated after 2 h incubations followed by resuspension of cells in new reaction media. (f) Endpoint concentrations of 1b and 1c as a function of reaction composition at our chosen time point of 24 h using "WC2" (cells transformed to express cvTA). Resting cells were incubated at 30 °C in 0.1 M HEPES pH 7.5 with 4x *i*Pr-NH_2 and 2 mM PLP. (g) Time-course kinetics of the reversible reductive amination of 1b to 1c catalyzed by cvTA, which reached a maximum conversion around 4 h. (h) Demonstration of WC2 reusability in rounds of batch catalysis initiated after 4 h incubations followed by resuspension of cells in new reaction media. Data shown are the average of n=3 trials with an error displayed as standard deviation. Null sign indicates no detectable traces were observed.

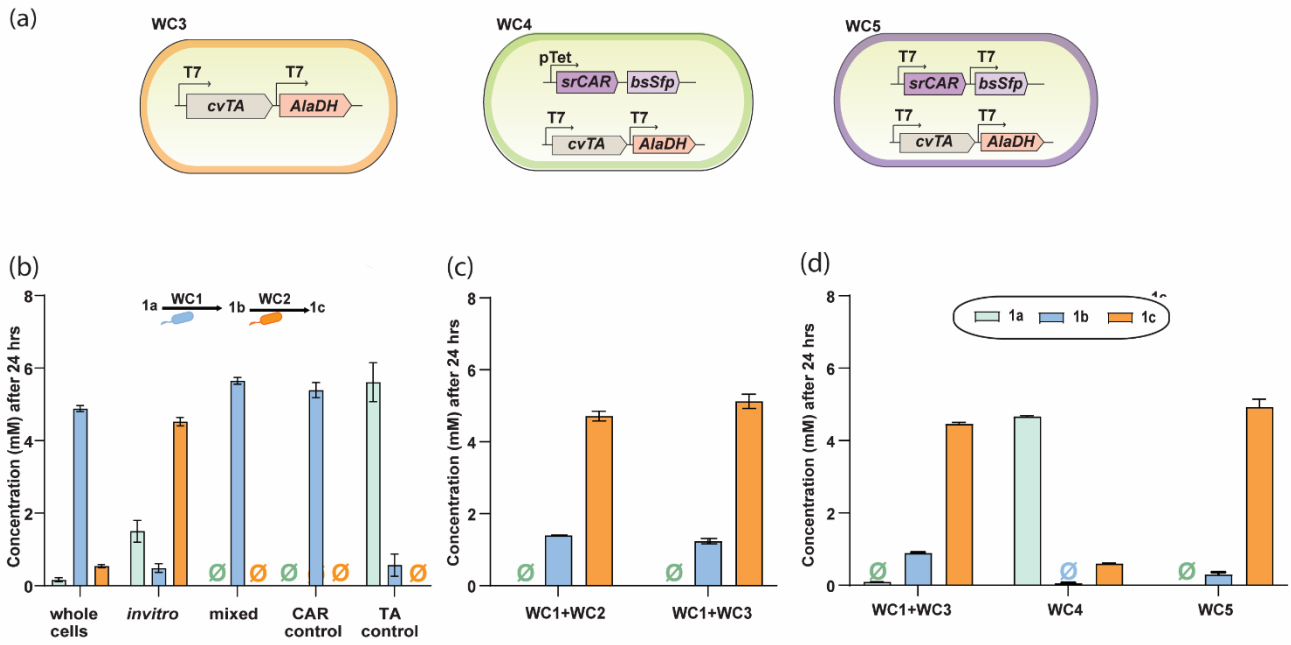

Figure 4. One-pot transformations of 1a to 1c using various whole-cell catalyst genotypes and conditions. (a) Illustrations of whole cell catalysts investigated – those that express srCAR and an associated activating enzyme bsSfp, cvTA, and AlaDH, or srCAR/bsSfp/cvTA/AlaDH all in one strain under different plasmid and promoter systems. The whole cells were incubated in a reaction buffer containing 0.1 M HEPES (pH 7.5), 10-110 mM glucose for cofactor regeneration, 10 mM $Mgcl_2$, 2 mM PLP, and 4-8x *i*Pr-NH_2. CAR control depicts the reaction mixture containing only WC1. (b) Comparison of endpoint measurements for one-pot 1a to 1c transformations indicates the poor performance of unoptimized whole cell format, particularly in the aldehyde to amine transformation step, when compared to purified enzyme format. (c) Improved conversion of 1a to 1c observed after optimization of reaction conditions showed greater than 80% yield (see panel S3 a-b). (d) Influence of the whole cell catalyst genotype on the endpoint concentration of amine synthesis.

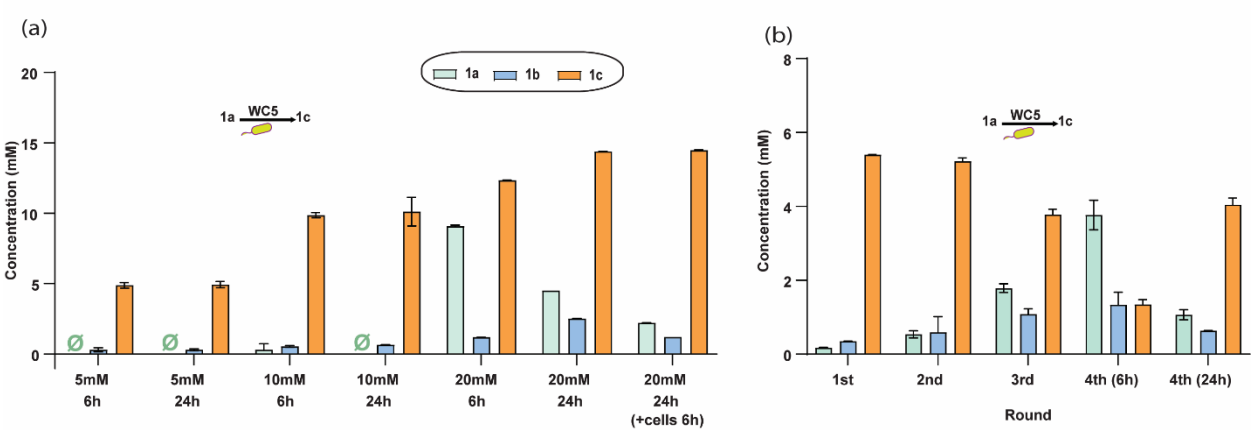

Figure 5. Evaluation of substrate tolerance, and reusability on WC5 whole cell biocatalyst. (a) Investigation of the optimized one-pot whole-cell cascade as a function of substrate loading and time. (b) Whole-cell biocatalyst reusability for the one-pot 1a to 1c bioconversion demonstrated that cells can be reused for at least 4 cycles without significant loss in reaction yield.

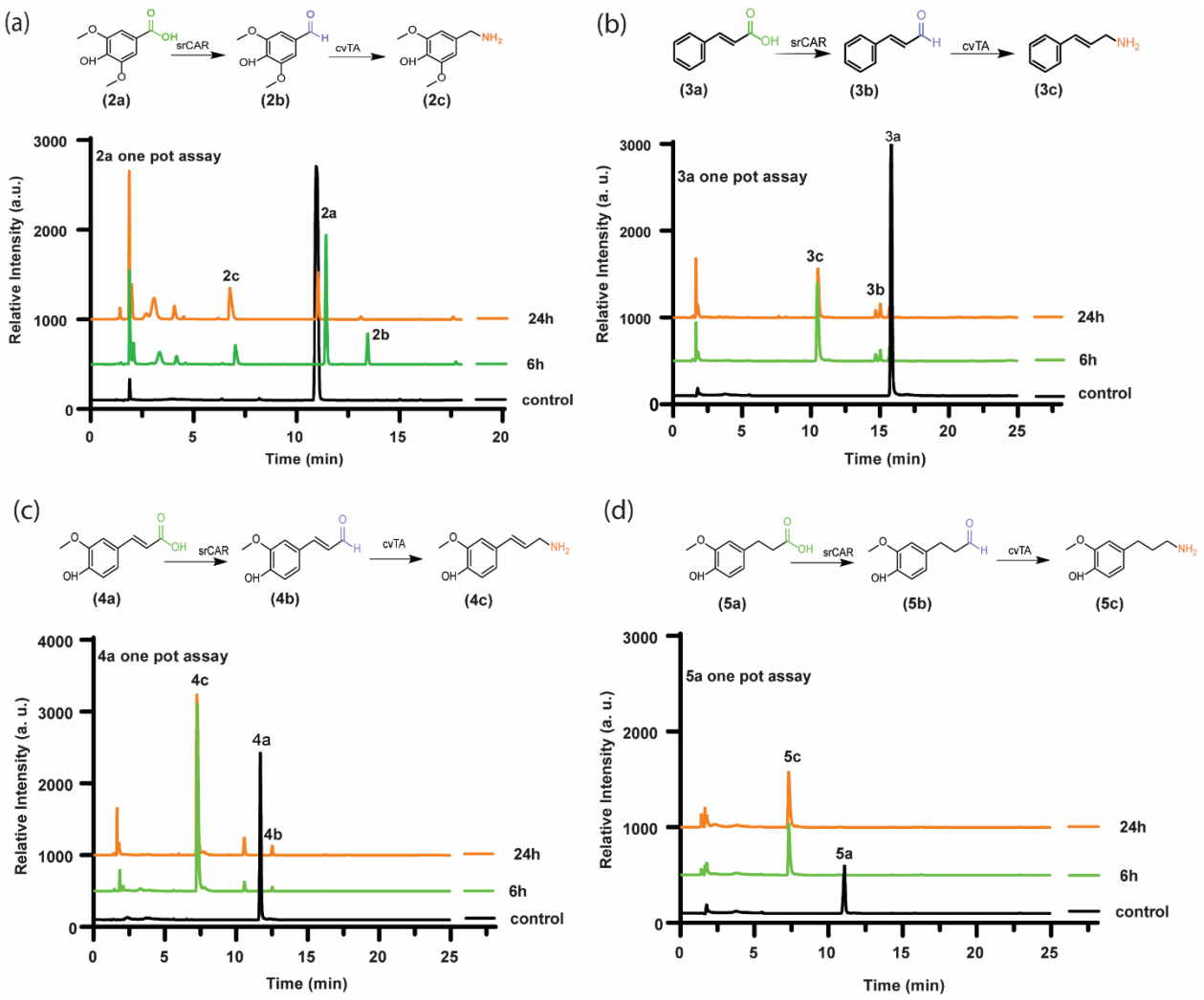

Figure 6. HPLC chromatogram traces of whole-cell, one-pot bioconversions of lignin-derivable carboxylic acids to heterocyclic primary amines. The traces show a control under reaction conditions for 24 h without whole cell addition (black) and one-pot assay samples after 6 h (green) and 24 h (orange). To synthesize these versatile amines, resting whole cell biocatalysts of WC5 (100 mg/mL wcw) containing overexpressed srCAR, bsSfp, cvTA, and AlaDH were incubated in 0.1 M HEPES at 30 °C, supplemented with 10 mM of glucose, 8x *i*Pr-NH_2, 10 mM $MgCl_2$, 10x NH_4Cl, 10% DMSO, and 2 mM PLP at 5 mM of 2a, 3a, 4a, or 5a substrate loading. In all the cases, control involved a 24 h reaction mixture without whole cells. (a) HPLC traces showing the control, 6 h, and 24 h results of the 2a one-pot assay, indicating the 2c formation however the yield is low (the whole cell, in this case, was harvested P2 expression conditions). (b) HPLC traces depicting the control, 6 h, and 24 h results of the 3a one-pot assay, demonstrating the high efficiency of the

whole cell biocatalyst system in converting 3a to 3c, resulting in a high yield of the product within 6 h. (c) HPLC traces of control, 6 h, and 24 h results demonstrate effective conversion of 4a to 4c. (d) HPLC traces of a 5a one-pot assay show highly efficient conversion of 5a to 5c within 6 hours, with complete consumption of the substrate and no detectable byproducts; the only peak observed corresponds to the desired product, 5c.